

Alicyclic photoresists for CO₂-based next-generation microlithography: A tribute to James E. McGrath

Mary Kate Boggiano^a, David Vellenga^d, Ruben Carbonell^c, Valerie Sheares Ashby^{a,1,*},
Joseph M. DeSimone^{a,b,c,*}

^a Department of Chemistry, University of North Carolina, CB #3290, Chapel Hill, NC 25499, USA

^b Department of Pharmacology, University of North Carolina, CB #3290, Chapel Hill, NC 25499, USA

^c Department of Chemical and Biomolecular Engineering, North Carolina State University, Partners I, Suite 3500, Raleigh, NC 27695, USA

^d Department of Electrical and Computer Engineering, North Carolina State University, Partners I, Suite 3500, Raleigh, NC 27695, USA

Available online 22 March 2006

Professor Jim McGrath has blended creativity with practicality and depth to produce a legacy in polymer science and education that we are privileged to celebrate in this issue. When we look at our students who work in Chapel Hill and the research that we conduct, we cannot help but see the ‘McGrath way’ in it all. His ability and desire to lead science and students in uncharted exciting directions is something that we strive to emulate. It is rare to find a scientist of Jim’s caliber who continues to see his success in the context of his students’ accomplishments. It is a pleasure for us to participate in this issue honoring him as he continues to play such a significant role in guiding his students, their students, and their students educationally and personally. As an example of Professor McGrath’s influence, his interest in microelectronics materials has successfully spanned at least one generation to the works described by previous members of the DeSimone group [1,2], as well as in the work described herein. Congratulations to Professor McGrath.

Abstract

Addition polymerization of norbornene-based monomers has been pursued toward the fabrication of photoresists for next-generation microlithography, using condensed carbon dioxide as the developing solvent. Addition polymers containing a norbornyl backbone, for dry plasma etch resistance and high thermal stability, were synthesized to include fluorinated moieties and chemical amplification switching groups. These materials have been characterized and their lithographic properties evaluated. Solubility differences between exposed and non-exposed resist have been observed in these novel systems, which should provide the necessary contrast for high-resolution imaging. Lithographic imaging produced dense lines as small as 3 μm.

© 2006 Elsevier Ltd. All rights reserved.

Keywords: Condensed CO₂; Addition polymerization; Photoresist synthesis

1. Introduction

In the drive for smaller image sizes in microelectronic devices, the lithography industry has reached a point where the solvents traditionally used for development have been shown to induce image collapse, caused by the high surface tension of the aqueous developer [3]. The use of a more gentle solvent, such as liquid and supercritical carbon dioxide (scCO₂), has been shown to be a potential solution to this problem [3–6]. Carbon dioxide is an environmentally benign and easily

* Corresponding authors. Address: Department of Chemistry, University of North Carolina, CB #3290, Chapel Hill, NC 25499, USA. Tel.: +1 919 962 2216; fax: +1 919 962 5463.

¹ Tel.: +1 919 962 3663; fax: +1 919 962 2388.

E-mail addresses: ashby@email.unc.edu (V.S. Ashby), desimone@unc.edu (J.M. DeSimone).

recyclable alternative to the solvents currently used in microlithography for the solvent-intensive steps of processing a photoresist. The low surface energy, low viscosity and high diffusivity of scCO₂ allow it to ‘wet’ all the surfaces of an image during development. Carbon dioxide can be vented from a wafer-processing chamber without the creation of a liquid–gas interface, helping to eliminate surface tension forces associated with traditional aqueous development that can lead to image collapse [7]. Carbon dioxide has been successfully used for development in conjunction with surfactants to remove aqueous developer without causing image collapse [6]. It has also been used in the absence of aqueous developer to obtain residue-free, high aspect ratio images [5]. Post-etch stripping has also been accomplished with CO₂-philic resists [1]. Advanced cluster tools can be envisioned using solvent-free processes, replacing traditionally wet steps with condensed CO₂ substitutes. The elimination of aqueous and solvent-based steps in photolithography could reduce processing time between tools, especially for transitions into dry

processes in vacuo. The use of condensed CO₂ in lithography could greatly reduce the costs of toxic waste disposal, as well as the costs of complying with environmental and health regulations.

As lithography continues with 193 nm technology, and considers future technologies, such as immersion and post-optical techniques, more stringent requirements are placed on the resist itself. The design criteria for photoresists to be used in CO₂ are well-aligned with the design criteria for 193 and 193 nm immersion resists. A stiff alicyclic backbone can impart etch resistance and elevate the glass transition temperatures of the resist. Fluorination has also been shown to decrease absorbance at shorter wavelengths [8]. The hydrophobicity of a highly fluorinated resist should also help prevent resist leaching into water, currently the leading choice among 193 nm immersion fluids. As an additional advantage for processing in CO₂, fluorination also increases CO₂ solubility, thereby offering a route to using highly fluorinated photoresists without requiring hydrophilic or lyophilic groups for adequate dissolution rates in traditional lithography solvents.

Given the requirements for modern photoresists and the goals of our group to incorporate condensed CO₂ as a processing solvent for lithography, copolymers of 1*H*,1*H*-perfluorooctyl methacrylate and tetrahydropyranyl methacrylate have previously been used in an entirely solvent-free process [2a]. Unfortunately, these materials lacked the adequate plasma etch resistance needed to protect the underlying substrate, etching at 2.5 times the rate of Shipley 1813 Novolac resist, in the presence of an oxidizing plasma [9]. Also, these methacrylate-based photoresists exhibited glass transition temperatures that were too low for typical baking steps in lithography. A promising approach to remedy these shortcomings, while maintaining the desired high CO₂ solubility, was to examine norbornene-based polymers with highly fluorinated side groups. The alicyclic backbone of norbornene addition polymers were predicted to impart slower etching rates than the corresponding methacrylate materials, based on the predictions of both the Ohnishi parameter [10] and the ring parameter [11]. Further, the use of a norbornene addition polymer was expected to provide a high glass transition temperature, as the polymer backbone would be much more highly strained than that of a methacrylate material. The fluorinated polymers were synthesized and examined for lithographic properties.

2. Experimental

2.1. Materials

Unless otherwise noted, all reagents were used as received. 1*H*,1*H*-Perfluorooctyl acrylate (FOA) was kindly received from 3M Co. It was distilled to remove inhibitor, then stored at 0 °C. Methylene chloride (analytical reagent grade) was purchased from Fisher Scientific and degassed with Ar. 3-(Norbornyl)-1,1,1-trifluoro-2-tri-(fluoromethyl)propan-2-ol (NBHFA) was purchased from Central Glass. SFC purity CO₂

was obtained from Air Products. Allylpalladium chloride dimer was purchased from Strem Chemicals. Diphenyl-*p*-tolylsulfonium triflate (WPAG) was kindly received from Wako Chemicals. 1,1,1,3,3-Pentafluorobutane was purchased from Solvay Fluorides under the trade name Solcane. All other reagents were purchased from Aldrich Chemical Co. Dicyclopentadiene was distilled immediately prior to use.

2.2. Characterization

¹H (399.9 MHz) and ¹⁹F NMR spectra were obtained on a Bruker Avance spectrometer; ¹H chemical shifts were referenced to CHCl₃ and ¹⁹F chemical shifts were referenced to α,α,α-trifluorotoluene (TFT). Infrared spectra were measured on a Perkin–Elmer Spectrum BX spectrometer from 4000 to 400 cm⁻¹. Thermogravimetric analyses were measured on a RTD 220 from Seiko Instruments up to 560 °C. Differential scanning calorimetry measurements were obtained on a DSC 220c from Seiko Instruments up to 250 °C at 10 °C/min. Elemental analyses were obtained through Atlantic Microlabs, Inc. Solubility measurements in CO₂ were determined using a stainless steel, high-pressure variable-volume view cell with a sapphire window. Intrinsic viscosity measurements were obtained from polymer solutions in TFT at 25 °C. Plasma etch data was obtained on a Semigroup 1000TP RIE tool at 20 °C, 100 W voltage, 60 mTorr operating pressure, and using a mixture of 5 sccm O₂ and 20 sccm CHF₃ as the etchant mixture. Lithography was performed on an ASML PAS 5500/950B 193 nm scanner, followed by development using condensed liquid CO₂.

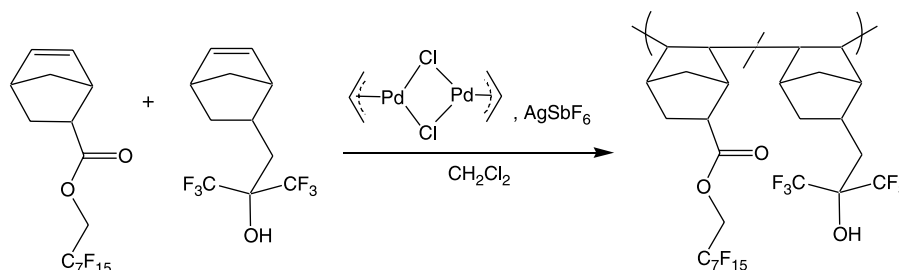
2.3. Synthesis

2.3.1. Synthesis of NBFOA

A pressure tube was charged with cyclopentadiene (4.40 g, 66.57 mmol), FOA (29.71 g, 65.42 mmol), and di-*tert*-butylphenol (68.4 mg, 0.33 mmol). The vessel was closed and heated to 170 °C for 2 days. Vacuum distillation at 80 °C afforded 31.64 g (93%) of a colorless liquid product. ¹H NMR (CDCl₃) ppm: 1.29 (br m, 1H, endo C3-endo position), 1.44 (br m, 2.9H, *exo* C3-*exo* position, *exo* C7, *endo* C7), 1.92 (m, 1.3H, *exo* C3-*endo* position and *endo* C2), 2.30 (m, 0.3H, *exo* C2), 2.91 (s, 1.3H, *endo* and *exo* C4 bridgehead), 3.02 (m, 1H, *endo* C3-*exo* position), 3.06 (s, 0.3H, *exo* C1 bridgehead), 3.22 (s, 1H, *endo* C1 bridgehead), 4.44 (q, 0.6H, *exo* CH₂-R_f), 4.59 (q, 2H, *endo* CH₂-R_f), [6.09, 6.14] (dd, 0.6H, *exo* vinyl), [5.89, 6.19] (dd, 2H, *endo* vinyl). ¹⁹F NMR (TFT) ppm: -71.90 (m, 0.6F, branched terminal CF₃), -80.89 (t, 3F, linear terminal CF₃), -119.46 (m, 2.5F, CF₂-CH₂), -122.03 (m, 4.5F, CF₂-CF₂-CH₂), -122.77 (br, 2.4F, CF₂-CF₂-CF₂-CF₃), -123.30 (br, 2.2F, CF₂-CF₂-CF₃), -126.17 (br, 2.1F, CF₂-CF₃). Anal. Calcd for C₁₆H₁₁O₂F₁₅: C, 36.92%; H, 2.12%; F, 54.81%. Found: C, 37.16%; H, 2.19%; F, 54.49%.

2.3.2. Synthesis of poly(NBFOA/NBHFA) I

A typical polymerization using a palladium catalyst was carried out in an inert atmosphere, similar to literature



Scheme 1. Synthesis of fluorinated addition copolymer of NBFOA and NBHFA.

procedures [12]. A solution of allylpalladium chloride dimer (24.6 mg, 67.2 μmol) and AgSbF_6 (50.4 mg, 146.8 μmol) in CH_2Cl_2 (5 mL) was stirred for 10 min. The catalyst solution was transferred via cannula onto a ground glass frit and allowed to drip into a flask containing NBFOA (2.446 g, 4.703 mmol) and NBHFA (0.563 g, 2.055 mmol). The yellow reaction mixture was heated to reflux for 3 h. The resultant gelatinous yellow solid was purified via washing with Celite and carbon black. Precipitation into hexanes yielded 1.912 g (64%) of a white powder. ^1H NMR (CDCl_3) ppm: [0.60–3.17] (br, 13.3H), [4.00–5.00] (br, 2H, $\text{CH}_2\text{-R}_f$). ^{19}F NMR (TFT) ppm: –72.93 (m, 0.6F, branched terminal CF_3), [–76.40 to –79.30] (br, 2F, NBHFA), –82.16 (s, 3F, linear terminal CF_3), –120.20 (br, 1.7F, $\text{CF}_2\text{-CH}_2$), –122.69 (m, 3.7F, $\text{CF}_2\text{-CF}_2\text{-CF}_2\text{-CH}_2$), –123.55 (br, 1.8F, $\text{CF}_2\text{-CF}_2\text{-CF}_2\text{-CF}_3$), –124.14 (br, 0.5F, $\text{CF}_2\text{-CF}_2\text{-CF}_3$), –127.08 (br, 1.8F, $\text{CF}_2\text{-CF}_3$). IR (neat on NaCl) cm^{-1} : [3180–3550] (br, NBHFA alcohol), 2955 (str, CH_2), 2880 (med, CH), 1748 (str, NBFOA C=O). Anal. Calcd for 70% ($\text{C}_{16}\text{H}_{11}\text{O}_2\text{F}_{15}$)/30% ($\text{C}_{11}\text{H}_{12}\text{OF}_6$): C, 39.00%; H, 2.53%; F, 52.38%. Found: C, 38.69%; H, 2.52%; F, 52.78%. DSC: T_g at 120 $^\circ\text{C}$. TGA (N_2): 5 wt% loss at 330 $^\circ\text{C}$. Intrinsic viscosity: 2.58 mL/g.

2.3.3. Protection of **1** with *t*-butoxycarbonate **2**

Polymer modification was carried out similar to literature procedures [13]. A solution of **1** (30 mol% NBHFA, 1.248 g, 0.839 mmol –OH) in Solcane (15 mL) was charged with di-*tert*-butyldicarboxylate (0.298 g, 1.364 mmol), followed by addition of *N,N*-dimethylaminopyridine (0.178 g, 1.439 mmol). The pale yellow solution turned brown and was stirred at room temperature for 18 h. The product was isolated via precipitation into hexanes, followed by precipitation into methanol, yielding 1.003 g (75%). ^1H NMR (CDCl_3) ppm: [0.56–3.64] (br, 1.45 (br, *t*BOC) [4.04–5.10] (br, $\text{CH}_2\text{-R}_f$). ^{19}F NMR (TFT) ppm: –72.93 (br, branched terminal CF_3), [–70.96 to –74.21] (br, NBHFA-*t*BOC), –81.99 (s, 3F, linear terminal CF_3), –120.02 (br, 1.4F, $\text{CF}_2\text{-CH}_2$), –122.27 (m, 3.5F, $\text{CF}_2\text{-CF}_2\text{-CF}_2\text{-CH}_2$), –123.11 (br, 1.4F, $\text{CF}_2\text{-CF}_2\text{-CF}_2\text{-CF}_3$), –123.69 (br, 0.4F, $\text{CF}_2\text{-CF}_2\text{-CF}_3$), –126.65 (br, 1.8F, $\text{CF}_2\text{-CF}_3$). IR (neat on NaCl) cm^{-1} : 2955 (str, CH_2), 2880 (med, CH), 1765 (str, *t*BOC C=O), 1757 (str, NBFOA C=O). Anal. Calcd for 70% ($\text{C}_{16}\text{H}_{11}\text{O}_2\text{F}_{15}$)/30% ($\text{C}_{16}\text{H}_{20}\text{O}_3\text{F}_6$): C, 40.32%; H, 2.88%; F, 49.08%. Found: C, 40.76%; H, 3.01%; F, 48.63%. DSC: T_g at 120 $^\circ\text{C}$. TGA (N_2): 6.1 wt% loss at 228 $^\circ\text{C}$; 10 wt% loss at 324 $^\circ\text{C}$. Intrinsic viscosity: 3.25 mL/g.

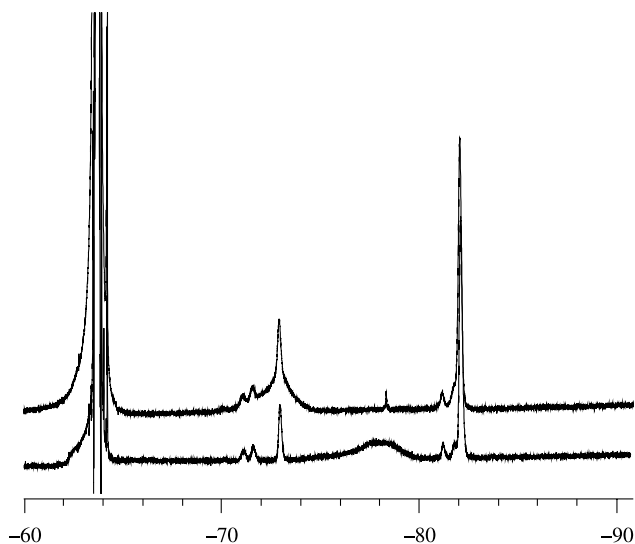
2.4. Lithography sample preparation

A photoresist formulation of 10 wt% **2** in TFT with 3 wt% WPAG was filtered four times through a 0.2 μm PTFE syringe filter. This solution was spin coated onto a 150 mm silicon wafer, followed by a 120 s bake at 105 $^\circ\text{C}$. Film thicknesses of approximately 400 nm were measured on a Tencor Alpha Step 200 Profiler, with a stylus force of 5 mg. Lithographic images were obtained on an ASML PAS 5500/950B scanner at the Triangle National Lithography Center, with NA = 0.63.

3. Results and discussion

The goal of this research was to make highly fluorinated, thermally stable copolymers, followed by lithographic evaluation of these materials with CO_2 development. A fluorinated norbornenyl monomer was initially synthesized by a Diels–Alder reaction of cyclopentadiene with a fluoroalkyl acrylate. A 1:3 mixture of *exo* and *endo* isomers was observed by ^1H NMR for NBFOA. The successful synthesis of NBFOA was also confirmed by elemental analysis.

Addition copolymers of NBFOA and NBHFA were synthesized using an allylpalladium dimer catalyst (Scheme 1). ^1H NMR and ^{19}F NMR of these polymers yielded expected results, based on spectroscopic comparison with the monomers. Protection of the hexafluoroalcohol group with *t*BOC

Fig. 1. ^{19}F NMR of **2** (top), and **1** (bottom). Expansion of the trifluoromethyl region.

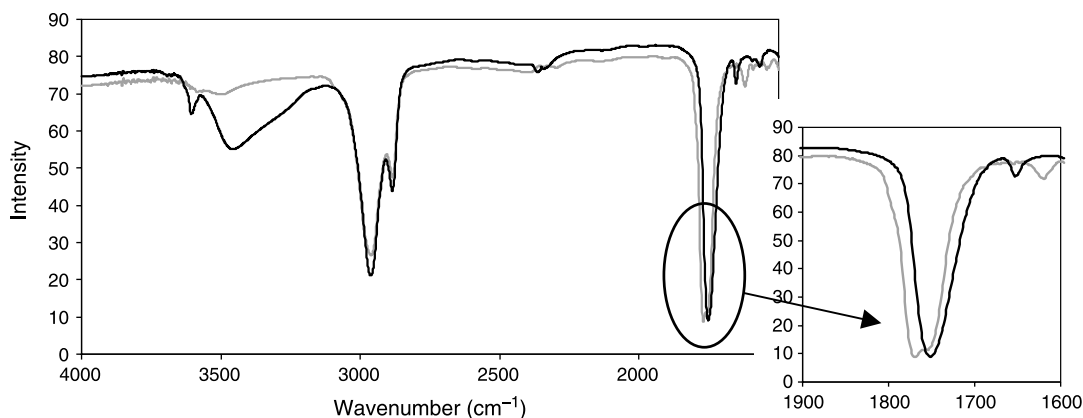


Fig. 2. Infrared spectra of the **2** (gray) and **1** (black) copolymers.

exhibited an upfield shift from -78 to -73 ppm in the ^{19}F NMR resonance corresponding to the trifluoromethyl groups adjacent to the protected alcohol (Fig. 1). The large resonance at -63 ppm is due to the TFT reference. The sharp resonances at -81 and -73 ppm are due to the terminal CF_3 groups in linear and branched NBFOA, respectively, [1,14]. Infrared spectroscopy also showed distinct differences between the protected and non-protected polymer. The broad OH stretch between 3550 and 3120 cm^{-1} was found to diminish after the OH group in the NBHFA monomer was protected with *t*BOC (Fig. 2). Also, the carbonyl stretch at 1749 cm^{-1} for the non-protected polymer is shifted slightly to 1756 cm^{-1} and a second, overlapping carbonyl stretch appears at 1764 cm^{-1} , indicating the presence of the second carbonyl from the *t*BOC group. Ultraviolet exposure of a polymer film containing 5 wt% triphenylsulfonium triflate successfully replicated the NMR and IR data of the non-protected polymer.

The polymers were soluble in liquid and condensed CO_2 as well as fluorinated solvents, with a significant difference in CO_2 solubility, thus providing an accessible region for CO_2 development (Fig. 3). The cloud point curves indicate regions of CO_2 pressure and temperature where the polymers are soluble in CO_2 . The materials are each soluble above the curve, and insoluble below the curve. Thus, this material is expected to act as a negative tone resist in CO_2 .

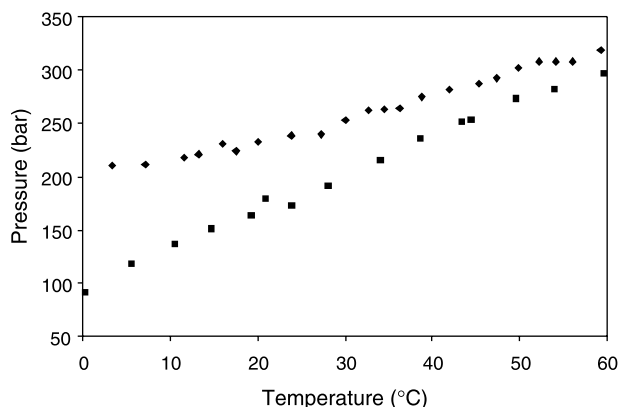


Fig. 3. Cloud point curves of **1** (◆), **2** (■). Both curves obtained at 2.5 wt% polymer in CO_2 .

Thermal gravimetric measurements were obtained on both **1** and **2** (Fig. 4). In polymer **1**, 5 wt% polymer degradation occurred above 300 °C , indicating excellent thermal stability of the non-protected polymer. In polymer **2**, an initial loss of 6.1 wt% was observed from 190 to 228 °C , which is in good correlation with the calculated mass of *t*BOC of 6.3 wt%. This suggests the polymer will be robust to typical baking steps in lithography.

Differential scanning calorimetry measurements of **2** showed a T_g at 120 °C (Fig. 5). Further heating to 220 °C showed erratic behavior above 150 °C , which might be attributed to melting of crystalline regions. The T_g was confirmed by slowly cooling, then reheating the sample. Notably, further heating above 150 °C did not produce the erratic behavior previously observed, indicating a fully amorphous material. The erratic thermal behavior in the second heat may be attributed to loss of the *t*BOC group, which would be in agreement with the TGA analysis.

Reactive ion etching was performed in an atmosphere of 5 sccm O_2 and 20 sccm CHF_3 (Fig. 6). Since this material was designed to be a negative-tone resist with CO_2 development, the non-protected material **1** would remain after development. Therefore, **1** was tested for its plasma etch rate. This polymer etched at 1.45 times the rate of a Shipley Novolac resin. Given that methacrylate-based 193 nm resists can etch at approximately twice the rate of Novolac in similar oxide etch processes [15], this system provides comparable etch resistance relative to methacrylate resists. The dry etch rate of this

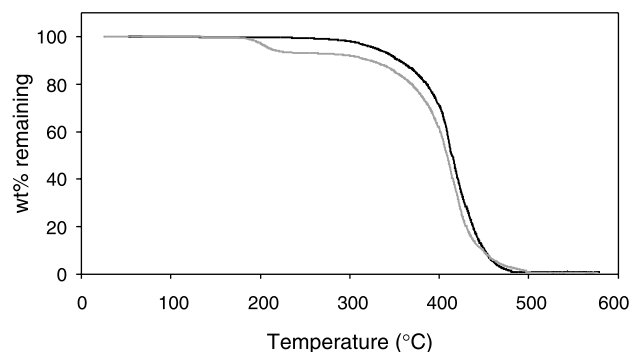


Fig. 4. Thermal gravimetric measurements of polymers **1** (black) and **2** (gray).

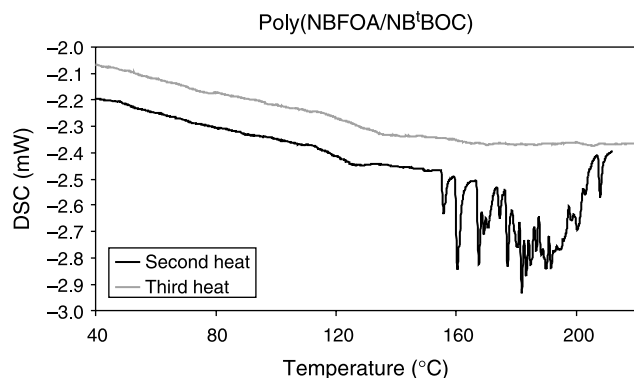


Fig. 5. Differential scanning calorimetry of **2**. Second heating to 220 °C shows erratic behavior above 150 °C. Cooling the sample, followed by a third heating, shows no erratic behavior.

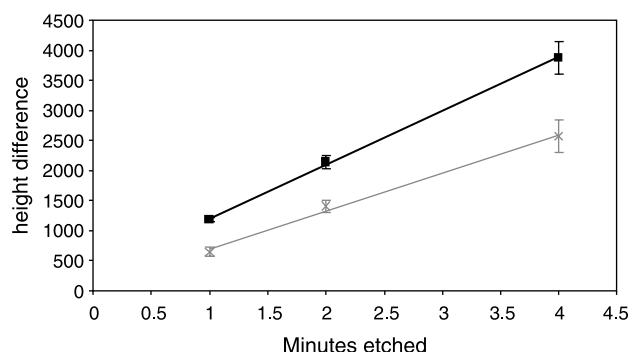


Fig. 6. Plasma reactive ion etching of Novolac (gray), **1** (black).

material may have been faster than expected, due to the high fluorine content of the polymer. Free fluorine radicals have been shown to increase plasma etch rates of organic materials [16]. Future work on this polymer platform may produce a material that sufficiently balances the fluorine content needed

for CO₂ solubility and a minimization of the etch rate. Further optimization of the etch rate may also be realized through on-going work exploring various etch gas compositions.

Initial images were obtained from a resist formulation of **2** and WPAG using a 193 nm ASML scanner. The latent images were developed in compressed CO₂ at 135 bar for 5 min with a dynamic flow of CO₂ through a backpressure regulator, set at 20 psi. The resultant images were observed by optical microscopy and SEM (Fig. 7). Images smaller than 3 μm could not be resolved without significant line edge roughness. This limitation may be due to several factors, including the high molecular weight of the polymer. The exact molecular weight of the material could not be determined, as the polymer was insoluble in standard gel permeation chromatography solvents, and ¹H NMR end group analysis could not be used, as the propyl end group resonances overlapped with the aliphatic norbornyl protons' resonances. However, the intrinsic viscosity of **2** was 3.25 mL/g, suggesting a high molecular weight. The linewidth resolution of a polymer can be limited by the radius of gyration (R_g) of the polymer. This effective 'pixel size' decreases as the R_g of the polymer decreases, which decreases with molecular weight. The other major factor preventing the resolution of smaller linewidths could be acid diffusion due to post exposure delay. Given the non-conventional CO₂ development, significant post exposure delay was inevitable, with the time needed to cleave the exposed wafer and pressurize the CO₂ cell.

4. Conclusion

Recent efforts toward the synthesis of viable resists for 'solvent-free' CO₂-based lithography have focused on norbornene-based addition polymers. These materials exhibit high thermal stability and CO₂ solubility. Further work on these materials will examine DUV absorbances and the control of molecular weight to promote solubility differences in CO₂ as well as in TMAH.

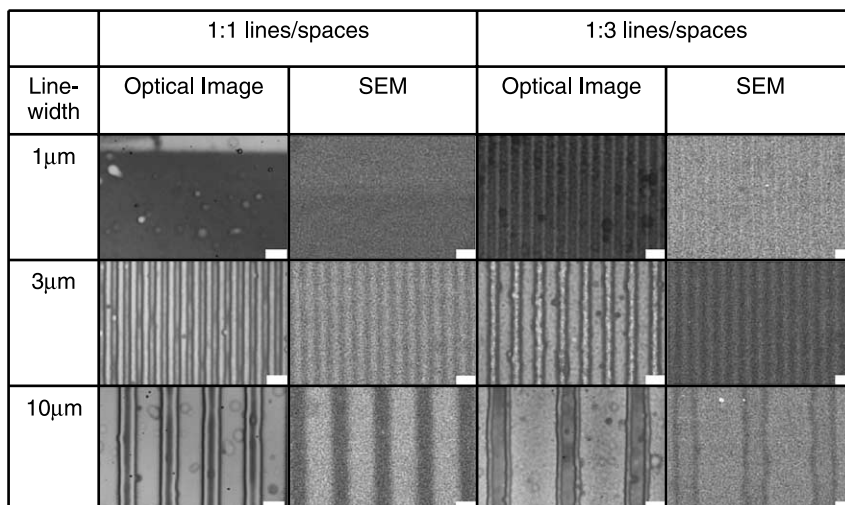


Fig. 7. Images obtained using the norbornene-based photoresist and CO₂-development. (a) Optical microscopy, and (b) SEM of the same die. Scale bar is 10 μm.

Acknowledgements

This work would not have been possible without the help of the TNLC staff at NCSU. Funding for this project has been generously provided by The NSF-STC for Environmentally Responsible Solvents and Processes. This material is based upon work supported in part by the STC program of the National Science Foundation, under agreement No. CHE-9876674.

References

- [1] Hoggan EN, Kendall JL, Flowers D, Carbonell RG, DeSimone JM. *Polym Mater Sci Eng* 1999;81:47–8.
- [2] (a) Hoggan EN, Wang K, Flowers D, DeSimone JM, Carbonell RG. *IEEE Trans Semicond Manuf* 2004;17(4):510–6.
(b) Zannoni LA, Simhan J, DeSimone JM. *Proc SPIE (Adv Resist Technol Process)* 2003;5039(2):1327–32.
(c) Denison GM, Jones III C, DeYoung J, Gross S, McClain J, Zannoni LA. *PMSE Prepr* 2004;90:152–3.
- [3] Simons JP, Goldfarb DL, Angelopoulos M, Messick S, Moreau WM, Robinson C, et al. *Proc SPIE (Adv Resist Technol Process)* 2001;4345(1):19–29.
- [4] (a) McAdams CL, Flowers D, Hoggan EN, Carbonell RG, DeSimone JM. *Proc SPIE (Adv Resist Technol Proc)* 2001;4345(1):327–34.
(b) Gallagher-Wetmore P, Wallraff GM, Allen RD. *Proc SPIE* 1995;2438:694–708.
- [5] Sundararajan N, Yang S, Ogino K, Valiyaveettil S, Wang J, Zhou X, et al. *Chem Mater* 2000;12:41–8.
- [6] Goldfarb DL, de Pablo JJ, Nealey PF, Simons JP, Moreau WM, Angelopoulos M. *J Vac Sci Technol B* 2000;18(6):3313–401.
- [7] (a) DeYoung JP, McClain JB, Gross SM. US Pat Appl 2002112746.
(b) DeYoung JP, McClain JB, Gross SM, DeSimone JM. US Pat Appl 2002112740.
- [8] Kunz RR, Bloomstein TM, Hardy DE, Goodman RB, Downs DK, Curtin JE. *J Vac Sci Technol B* 1999;17(6):3267–72.
- [9] Flowers D. Designing photoresist systems for dry microlithography in carbon dioxide. University of North Carolina Dissertation; 2002.
- [10] Gokan H, Esho S, Ohnishi Y. *J Electrochem Soc* 1983;130(1):143–6.
- [11] Kunz RR, Palmateer SC, Forte AR, Allen RD, Wallraff GM, DiPietro RA, et al. *Proc SPIE (Adv Resist Technol Process)* 1996;2724:365–76.
- [12] Okoroanyanwu U, Shimokawa T, Byers JD, Willson CG. *J Mol Catal A* 1998;133:93–114.
- [13] Tran HV, Hung RJ, Chiba T, Yamada S, Mrozek T, Hsieh Y-T, et al. *Macromolecules* 2002;35(17):6539–49.
- [14] Resnick P. Personal communication; 2005.
- [15] Wallow T, Brock P, DiPietro R, Allen R, Opitz J, Sooriyakumaran R, et al. *Proc SPIE (Adv Resist Technol Process)* 1998;3333(1):92–101.
- [16] Collart EJH, Baggerman JAG, Visser RJ. *J Appl Phys* 1995;78(1):47–54.